

## **UPDATE TO EXPERIMENT E91-003**

A Study of Longitudinal Charged Pion Electroproduction on  $H$ ,  $^2H$ ,  $^3He$  and  $^4He$

### **Submitted by**

J. Arrington, K. Bailey, F. Dohrmann, D. F. Geesaman, K. Hafidi,  
H. E. Jackson (SPOKESPERSON), T. O'Connor, P. E. Reimer,  
D. Potterveld, B. Zeidman

**Argonne National Laboratory, Argonne, IL 60439**

J. Reinhold

**Florida International University, Miami, FL 33199**

R. Carlini, R. Ent, A. Lung, D. Mack, G. Smith, W. Vulcan, S. Wood

**Jefferson Laboratory, Newport News VA 23606**

S. Avery, O. K. Baker, E. Christy, A. Gasparian, P. Gueye,  
B. Hu, C. Keppel, L. Tang

**Hampton University, Hampton VA 23668**

D. Gaskell, P. Welch

**Oregon State University, Corvallis, Or 97331**

R. Gilman, C. Glashauser

**Rutgers University, Piscataway, NJ 08855**

E. Kinney

**University of Colorado, Boulder, Co 80309**

R. J. Holt

**University of Illinois-Urbana, Urbana, Il 61801**

R. Asaturyan, H. Mkrtchyan, S. Stepanyan, V. Tadevosyan

**Yerevan Physics Institute, Armenia**

## Abstract

A series of measurements of single pion electroproduction on the proton, deuteron, and  $^3\text{He}$  was completed recently at Jefferson Laboratory by the NucPi Collaboration. The data form the first part of a study of longitudinal electroproduction in light nuclei. The goal is a determination of the longitudinal cross section in parallel kinematics by means of a Rosenbluth separation, and a search for target-mass dependent effects. Longitudinal pion electroproduction should be sensitive to nuclear pion currents because of the dominance of the pion-pole process for charged-pion emission in the direction of the virtual photon. The mass dependence of the longitudinal cross section should provide insight into the absence of any enhancement of sea quark distributions in nuclei as measured in deep-inelastic scattering. Data have been obtained at  $Q^2 = 0.4 \text{ GeV}^2$ , for  $W = 1.15$  and  $W = 1.6 \text{ GeV}$  from  $H$ ,  $^2\text{H}$ , and  $^3\text{He}$ , and for a range of values of  $Q^2$  on  $H$  and  $^2\text{H}$  at  $W = 1.95 \text{ GeV}$ . Results from the analysis of these data are discussed, and a run plan of 400 hours of beam for completing this study is presented.

## 1 Introduction

According to the simplest models of the nucleon-nucleon force, pion-exchange currents in nuclei should give rise to a mass-dependent enhancement<sup>1</sup> of the nuclear pion charge distribution. Longitudinal pion electroproduction should be sensitive to nuclear pion currents because of the dominance of the pion-pole process for charged-pion emission in the direction of the virtual photon. If current conceptions of pion-exchange currents in nuclei are correct, longitudinal electroproduction will be suppressed at lower momentum transfers and enhanced at higher momentum transfers. These currents should also manifest themselves in quark-antiquark distribution functions<sup>2,3</sup> as observed in deep-inelastic scattering(DIS) on nuclei. However, analysis of parton distribution functions shows no evidence for any nuclear enhancements of sea quarks. Recent data from Drell-Yan studies<sup>4</sup> which directly probe the antiquark sea, show no mass dependence. These results suggest that a reformulation of pion-exchange models of nuclear forces may be required. In an attempt to probe exchange currents directly, we have carried out a series of measurements of single-charged-pion electroproduction on the proton, deuteron, and  $^3\text{He}$  at TJNAF. The goal is to measure the longitudinal cross section in parallel kinematics by means of a Rosenbluth separation, and to search for target-mass dependent effects. The results from these measurements should provide insight into the absence of any enhancement of sea quark distributions in nuclei as measured in DIS.

E91-003 was approved for an initial phase of 500 hours to make measurements at two of the four kinematic configurations proposed and for four targets,  $H$ ,  $^2\text{H}$ ,  $^3\text{He}$ , and  $^4\text{He}$ . Because the shakedown and commissioning of the Hall C cryogenic target proved much more difficult than anticipated, only a portion of this program was completed in the initial run, but enough data was obtained with  $^2\text{H}$  and  $^3\text{He}$  to provide a useful examination of the mass dependence of the longitudinal cross sections. The data obtained and the details of the analysis of the data are the basis of the run plan presented here. This proposal will complete the experiment and provide a coherent examination of single charged electroproduction on light nuclei.

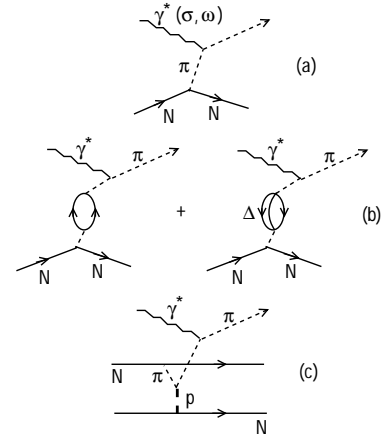
## 2 Measurements

The single  $\pi$  electroproduction cross section for the free proton has the form

$$\frac{d\sigma}{d\Omega_{e'} dE_{e'} d\Omega_{\pi}^*} = \Gamma \left[ \frac{d\sigma_t}{d\Omega_{\pi}^*} + \epsilon_l \frac{d\sigma_l}{d\Omega_{\pi}^*} + \sqrt{2\epsilon_l(1+\epsilon)} \frac{d\sigma_{lt}}{d\Omega_{\pi}^*} \cos\phi_{\pi}^* + \epsilon \frac{d\sigma_{tt}}{d\Omega_{\pi}^*} \cos 2\phi_{\pi}^* \right]$$

where  $\Gamma$  is the virtual photon flux,  $\epsilon$  is the transverse polarization and  $\epsilon_l = \frac{q^2}{\omega^2} \epsilon$  the longitudinal polarization of the virtual photon. The pion angles  $\theta_{\pi}^*$  and  $\phi_{\pi}^*$  are defined in the center-of-mass frame. For forward electroproduction, ie.  $\theta_{\pi}^* = 0$ , the pion pole process, which corresponds to scattering by the pion field, is known<sup>5</sup> to

Fig.1 *Electron charge scattering due to the nucleon pion field in lowest order(a) and from multinucleon higher order processes(b,c).*



to be the largest single process contributing to the longitudinal piece of the cross section. To the extent that the pole process dominates,  $\frac{d\sigma_l}{d\Omega_{\pi}^*}(\theta_{\pi}^* = 0)$  provides a direct probe of the basic  $N \rightarrow N\pi$  coupling. Multinucleon processes, which can be related to the nuclear pion excess will modify this cross section in nuclear targets. The pole process is shown in Fig. 1a, and the multinucleon processes which may modify the pole amplitude are shown in Fig. 1b,c. It is useful to view these effects as modifications of the elementary  $N \rightarrow N\pi$  coupling in nuclear matter. Consequently, a direct comparison of the longitudinal cross section per nucleon in the nuclear targets with the experimental value for the free nucleon will provide evidence for the presence of multinucleon effects which can be related to the nuclear pion excess. The deuteron and  $^3\text{He}$  are particularly interesting systems for which microscopic calculations of these multinucleon contributions may be possible. The measurements were carried out at Jefferson Lab in Feb-April 1998 using the Hall C facility. 0.845 to 3.245 GeV electrons were scattered from high-density cryo-targets. The scattered electrons were observed in the High Momentum Spectrometer in coincidence with pions observed in the Short Orbit Spectrometer. Additional data (on deuterium and hydrogen only), taken in the fall of 1997 during the running of E93-021 ( $F_{\pi}$ ), have also been analyzed in conjunction with the  $F_{\pi}$  collaboration. The kinematic conditions, shown in Table 1, correspond to virtual pion momenta ( $k_{\pi}$ ) for which, in one case, the electroproduction is expected to be quenched ( $k_{\pi} \approx 200 \text{ MeV}$ ), and a second, in which according to the standard pion-exchange model of nuclear forces, one expects a substantial enhancement

Table 1: Kinematic Conditions for JLAB experiment E91-003 (includes data taken during E93-021). Note that the units, here and throughout the text, assume  $c = 1$ .

E	$\omega$	$\Theta_e$	$\Theta_q$	W	$Q^2$	$P_\pi$	$\epsilon$	$k_\pi$
GeV	GeV	deg	deg	GeV	GeV <sup>2</sup>	GeV		GeV
0.845	0.46	66.87	27.11	1.150	0.396	0.327	0.43	0.451
1.645	0.46	26.04	41.94	1.150	0.396	0.327	0.86	0.451
1.645	1.108	39.33	15.46	1.600	0.400	1.079	0.49	0.197
3.245	1.108	13.79	23.54	1.600	0.400	1.079	0.89	0.197
2.446	1.879	38.40	10.01	1.950	0.600	1.856	0.37	0.180
3.549	1.879	18.31	14.87	1.950	0.600	1.856	0.74	0.180
2.669	1.957	36.60	11.45	1.950	0.750	1.929	0.43	0.210
3.549	1.957	21.00	15.47	1.950	0.750	1.929	0.70	0.210
3.007	2.410	56.33	10.50	1.950	1.600	2.326	0.27	0.400
4.045	2.410	28.49	16.63	1.950	1.600	2.326	0.63	0.400

( $k_\pi \approx 400 \text{ MeV}$ ) (see Fig. 2). In the forward direction only  $\frac{d\sigma_L}{d\Omega_\pi^*}$  and  $\frac{d\sigma_T}{d\Omega_\pi^*}$  contribute to  $\frac{d\sigma}{d\Omega_{e'} dE_{e'} d\Omega_\pi^*}$ . Measurements were made at kinematics corresponding to two virtual photon polarizations for each momentum transfer in order to carry out a Rosenbluth separation of the transverse and longitudinal cross sections. To date, measurements have been made for the proton, deuterium, and  $^3\text{He}$ . A direct comparison of the cross sections for each target measured in the identical geometry allows the determination of mass dependences to better precision than measurements of absolute cross sections.

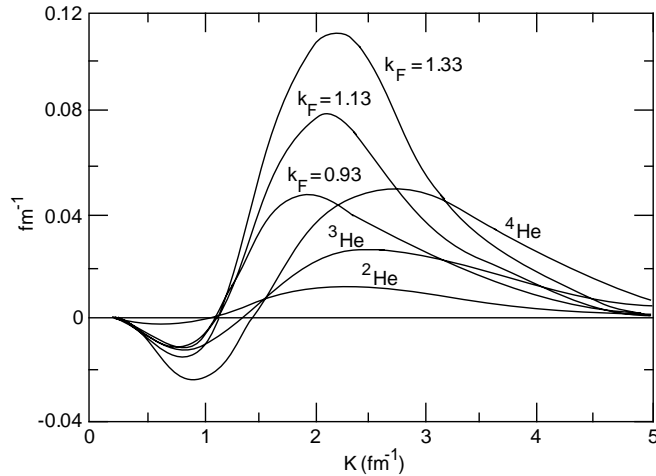


Fig. 2 Calculation of the pion excess as a function of  $k_\pi$  from Friman et al<sup>1</sup>. Data was taken during E91-003 at  $k_\pi \approx 1 \text{ fm}^{-1}$  and  $k_\pi \approx 2 \text{ fm}^{-1}$ .

### 3 Results

The general features of the deuterium and  ${}^3\text{He}$  pion spectra in missing mass are typical of quasifree pion electroproduction. An example of the data obtained is shown in Fig. 3

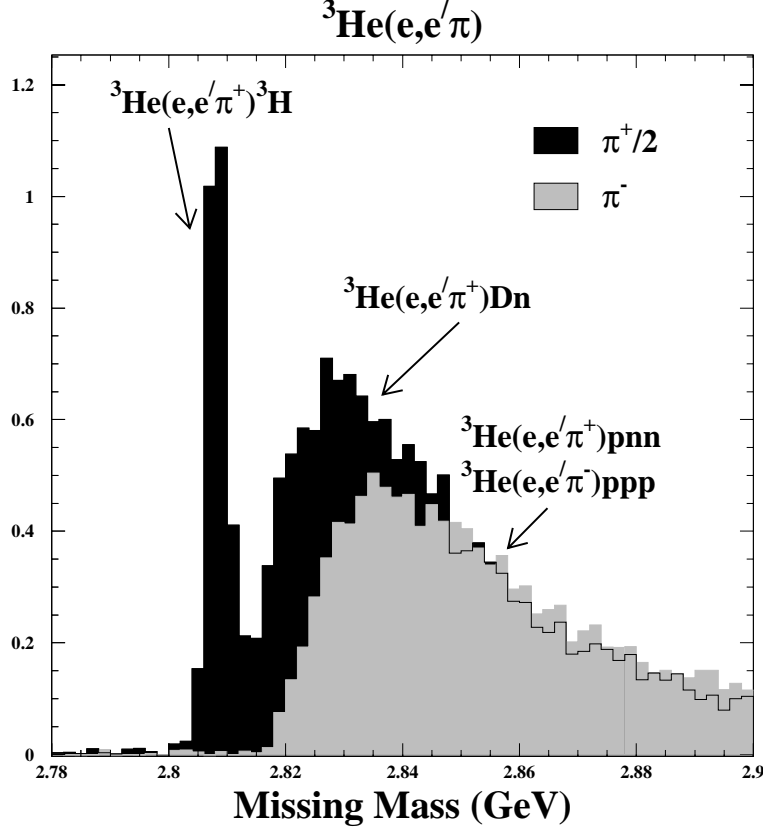


Fig. 3 *The Missing Mass Spectra for  $\pi^+$  and  $\pi^-$  electroproduction on  ${}^3\text{He}$  with  $W = 1.6$  GeV,  $Q^2 = 0.40$  GeV $^2$ .*

in which the missing mass spectra for  $\pi^+$  and  $\pi^-$  production on  ${}^3\text{He}$  are compared. The  $\pi^+$  yield was divided by 2 in order to make a direct comparison of the  $\pi^+$  production on the protons in  ${}^3\text{He}$  with  $\pi^-$  production on the neutron. For the  $\pi^+$  production, in addition to the quasifree component which appears to be the same as for  $\pi^-$ , there is a sharp peak corresponding to coherent production leading to a triton in the final state. In addition, there is a component corresponding to a deuteron and neutron in the final state. The forward angle electroproduction cross section integrated over missing mass,  $\frac{d^3\sigma}{d\omega d\Omega_e d\Omega_\pi} = \int \Gamma_v [\frac{d^2\sigma_t}{dM d\Omega_\pi} + \epsilon \frac{d^2\sigma_l}{dM d\Omega_\pi}] dM$  provides the most direct basis for comparing quasifree electroproduction with production on the free nucleon. The ratio of this cross section to that of the proton is a robust indicator of any mass dependence. Measurements of absolute cross sections are not necessary, and to first order corrections for decay-in-flight and pion detection efficiency cancel in the ratio. The ratio of the luminosity normalized pion yields corrected for experimental acceptance,  $\frac{d^3\sigma_A}{d^3\sigma_p} \equiv \frac{(N^{\pi^+}_A/q_A)/\text{exp\_accept}_A}{(N^{\pi^+}_p/q_p)/\text{exp\_accept}_p}$ , was used to estimate the cross section ratio. Unseparated cross section ratios measured for two invariant masses are presented in Table 2. The first kinematics correspond to a virtual pion momentum of 197 MeV in the region where a quenching of the cross section

is expected. The second kinematics correspond to 450  $MeV$  where an enhancement could occur. The data in Table 2 show an apparent quenching of the nuclear cross sections at each measured point. However, these data must be corrected for the trivial modification of the nuclear cross sections which comes from the kinematic effects of the Fermi momenta of the target nucleons. The physics quantity of basic interest is the longitudinal charged pion electroproduction cross section for the proton bound in the deuteron and  ${}^3He$  measured relative to the cross section for the free proton. To extract this quantity, the experimental measured coincidence yield is simulated in a Monte Carlo calculation (SIMC) using a realistic model of the experiment. The effects of spectrometer response, radiation, nucleon Fermi motion, and kinematic variation of the primary nucleon cross section are included in the simulation. The measured data are compared with the simulation. The input model cross section is refined and the process iterated until the best fit is obtained. The extracted experimental cross section is then defined as  $\sigma(Q_0^2, W_0, \Theta_{cm}) = \sigma_{model}(Q_0^2, W_0, \Theta_{cm}) * (data)/(SIMC)$ . To avoid corrections for the coherent contributions,  ${}^3He(e, e'\pi^+)T/Dn$ , to the  $\pi^+$  spectrum measured for  ${}^3He$ , the  $\pi^-$

Table 2: Unseparated cross section ratios for deuterium and  ${}^3He$

Kinematics	Target	$d^3\sigma_A^{\pi^+}/d^3\sigma_p$	$d^3\sigma_A^{\pi^-}/d^3\sigma_p$
$W = 1.6 GeV$	proton	1	
$\epsilon = 0.89$	deuteron	$0.85 \pm 0.04$	$0.83 \pm 0.04$
$k_\pi = 197 MeV$	${}^3He$	$(0.60 \pm 0.05)$	$0.59 \pm 0.04$
$W = 1.15 GeV$	proton	1	
$\epsilon = 0.86$	deuteron	$0.95 \pm 0.03$	$0.91 \pm 0.03$
$k_\pi = 451 MeV$	${}^3He$	$(0.79 \pm 0.03)$	$0.75 \pm 0.02$

spectrum corrected by the measured  $\pi^+$  to  $\pi^-$  ratio measured for  $\sigma_l$  in the deuteron is used to estimate quasifree  $\pi^+$  production in  ${}^3He$ . The resulting extracted cross section ratios (corrected for quasifree modifications to the nuclear cross sections) are shown in Fig. 4.

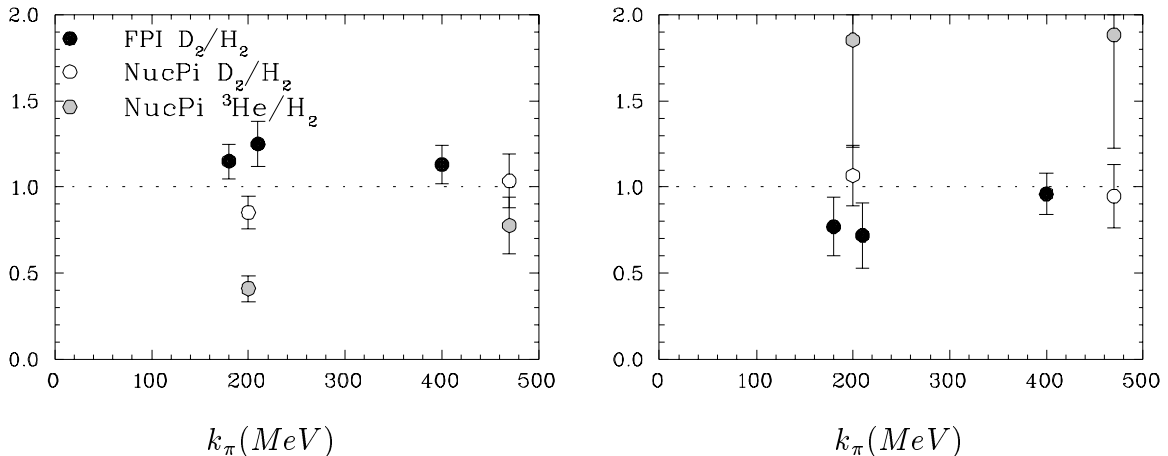


Fig. 4 The measured ratios of  $d\sigma_l/d\Omega_\pi$  and  $d\sigma_t/d\Omega_\pi$  for single  $\pi^+$  electroproduction on the deuteron and  ${}^3He$  to the free proton cross section

## 4 Discussion

Within the precision of the measurements summarized in Table 1, there is no clear signature of multinucleon contributions. The measured values of the  $d\sigma_l/d\Omega_\pi$  ratios cluster around one, with the exception of the point for  ${}^3\text{He}$  at 197 *MeV*. The transverse ratios for the deuteron also cluster near one, while the results for  ${}^3\text{He}$  are substantially greater than one. However, the errors for the latter points are unavoidably large because the corresponding  $d\sigma_t/d\Omega_\pi$  are small relative to  $d\sigma_l/d\Omega_\pi$ . There is no evidence in these data for a measurable enhancement of  $d\sigma_l/d\Omega_\pi$  in either target. The quenching observed in earlier measurements<sup>6</sup> on the deuteron at  $k_\pi = 200$  *MeV* is present in the deuteron data for  $W = 1.6$  *GeV* and appears stronger in  ${}^3\text{He}$ , ie  $\approx 0.4$ , but this trend is absent in the data at  $W = 1.95$  *GeV*. Qualitatively, these data are consistent with conclusions drawn from earlier work on DIS. There is no experimental evidence for a measurable pion excess. The absence of a measurable excess presents a major challenge to the conventional model of nuclear forces. Work on several fronts is necessary to make further progress in attacking this problem. First, a precise interpretation on the results presented here will require detailed theoretical estimates of the contributions expected from the exchange currents in the deuteron and  ${}^3\text{He}$ . Second, the sensitivity of our experiment should be substantially improved to make further progress. Third, it is important to extend the data to  ${}^4\text{He}$  for which the predicted pion excess approaches that of extended nuclear matter. It is also important to study the apparent discrepancy between measurements at  $W = 1.60$  *GeV* and  $W = 1.95$  *GeV* for  $k_\pi \approx 200$  *MeV*.

## 5 Experimental considerations

The first phase of E91-003 achieved much of its goal in obtaining high quality pion electroproduction data from light nuclei. Analysis of this data, however, has revealed some unforeseen complications that may affect the interpretation of the results. In particular, the  $W = 1.15$  *GeV* data set has revealed itself to be somewhat more complicated to deal with than anticipated. The sections that follow will discuss some of the relevant difficulties and demonstrate why the second phase of this experiment will be better accomplished at higher  $W$  (namely, 1.95 *GeV*).

### 5.1 Quasifree Correction

The goal of experiment E91-003 was to measure modifications to the longitudinal cross section to gain insight into nuclear pion currents. To that end, one must account for any spurious modifications of the cross section that have nothing to do with virtual pions in the nuclear medium. The most obvious such effect comes from the kinematic difference inherent in scattering a virtual photon from a stationary proton as opposed to a bound nucleon that has some momentum. Clearly, the total center of mass energy,  $W$ , will depend on the nucleon momentum and direction.

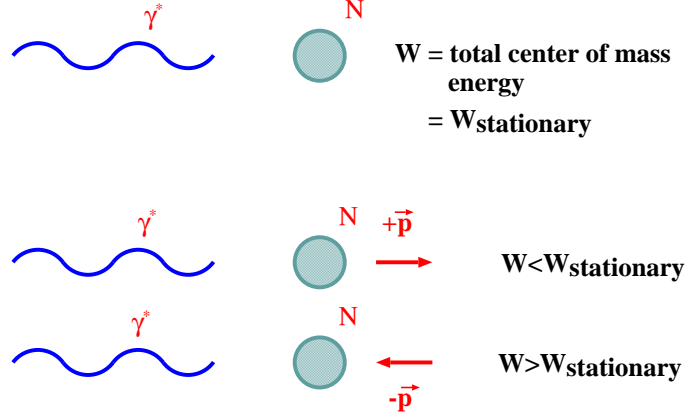


Fig. 5 *Cartoon of modification of center of mass energy ( $W$ ) due to nucleon momentum.*

The  $W$  dependence of the  $\gamma - N$  cross section leads one to conclude that, even in the absence of medium modifications, one does not necessarily expect the integrated nuclear cross section (per proton) to be equal to the proton cross section, i.e.,

$$\int \frac{d\sigma^A}{d\Omega dP_\pi} dP_\pi \neq \frac{d\sigma^H}{d\Omega}.$$

This effect was calculated and the resulting “quasifree correction” applied to the longitudinal ratios extracted from the E91-003 and E93-021 data sets.

Calculation of the above correction, already a somewhat model dependent quantity, can be further complicated at very low  $W$ . In this case, certain regions of the nucleon wave function result in a center of mass energy below pion production threshold and thus cannot contribute to the integrated cross section. This was an issue encountered in the analysis of the E91-003  $W = 1.15 \text{ GeV}$  data set. The additional correction due to this effect was estimated to be about 10% in deuterium.

At higher  $W$ , one can avoid the above threshold effects. While the quasifree modification to the cross section is still non-trivial, it is somewhat smaller. The situation is summarized in Table 3, where the E91-003  $W = 1.15 \text{ GeV}$  and  $W = 1.6 \text{ GeV}$  quasifree modifications in Deuterium are compared to the E93-021  $W = 1.95 \text{ GeV}$  modifications.

$W \text{ (GeV)}$	$Q^2 \text{ (GeV}^2\text{)}$	$k_\pi \text{ (GeV)}$	$(\sigma_L^D/\sigma_L^H)^{\text{quasifree}}$
1.15	0.4	0.45	0.80
1.60	0.4	0.20	0.97
1.95	1.6	0.40	0.90
1.95	0.6	0.20	0.94

Table 3: Modification of longitudinal cross section in Deuterium due to the Fermi motion of the bound nucleon. The modification is smaller at higher  $W$  due to the absence of threshold effects.



## 5.2 $P_\pi$ Coverage

One of the challenges in the analysis of the first phase of E91-003 has been the incomplete experimental acceptance of the pion momentum spectrum. In order to compare the nuclear targets to the free proton, the longitudinal cross section must be integrated over the detected pion momentum,  $P_\pi$  (or equivalently, missing mass). Namely, one would like to evaluate the ratio,

$$R_L = \left( \int \frac{d\sigma_L^D}{d\Omega_\pi dP_\pi} dP_\pi \right) / \frac{d\sigma_L^H}{d\Omega_\pi}.$$

While the coverage of the pion momentum distribution was very complete for the E91-003 low recoil ( $k_\pi = 200 \text{ MeV}$ ) and the E93-021 data sets, it was rather poor for the E91-003 high recoil ( $k_\pi = 450 \text{ MeV}$ ) data set (see Fig. 6).

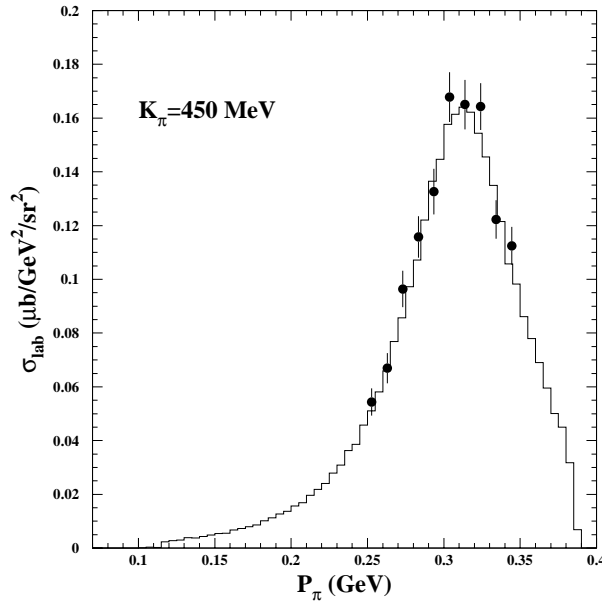


Fig. 6  $P_\pi$  distribution for  $D(e, e' \pi^+)$ . Experimental data (solid circles) is compared to a quasifree calculation that includes NN final state interaction effects.

There are two obvious ways to correct for this problem. The first would be to use a calculation to extrapolate the measured shape of the spectrum to the unmeasured regions, similar to what is shown in Fig. 6. This has the disadvantage of being highly sensitive to the model used in the calculation as well as possible NN final state interaction effects distorting the simple quasifree shape. The other alternative is to combine this  $P_\pi$  coverage correction with the quasifree correction mentioned in the previous section. In that case, one merely truncates the quasifree calculation to agree with the experimental acceptance. This alternative is also not ideal in that one is only probing the longitudinal strength over a portion of the  $P_\pi$  distribution. In particular, the longitudinal strength beyond the region of  $P_\pi$  accepted may deviate significantly from that predicted by the quasifree calculation.

Clearly, the ideal situation is one in which the full momentum spectrum is within the experimental acceptance. At higher pion momenta, one gains a larger absolute  $P_\pi$  acceptance for the same fractional momentum bite. This is exactly the situation in the higher momentum data from the first phase of this experiment, as well as for the data taken during E93-021 ( $F_\pi$ ). For example, simulations indicate that for the proposed kinematics, greater than 94% (in the worst case) of the  $P_\pi$  distribution from  ${}^3\text{He}$  can be sampled.

### 5.3 Pion-pole Dominance

To ensure that the E91-003 measurement is maximally sensitive to the nuclear pion field, the longitudinal production must proceed primarily via the pion pole term (Fig. 1a). In this picture, one can roughly view the process as being the product of the  $\gamma - \pi$  cross section modified by the probability to find a virtual pion with a given momentum ( $k_\pi$ ).

The ratio of longitudinal  $\pi^-$  to  $\pi^+$  production from deuterium can be used to test if the pole term does indeed dominate. The pole process proceeds only through isovector photons, while other terms contributing to the longitudinal cross section can proceed through both isoscalar and isovector photons. In terms of isovector and isoscalar amplitudes, the ratio of longitudinal cross sections can be written,

$$\frac{\sigma(\gamma^* n \rightarrow \pi^- p)}{\sigma(\gamma^* p \rightarrow \pi^+ n)} = \frac{|A_v - A_s|^2}{|A_v + A_s|^2}.$$

Provided that the relative phase does not conspire to mask the contribution of the isoscalar

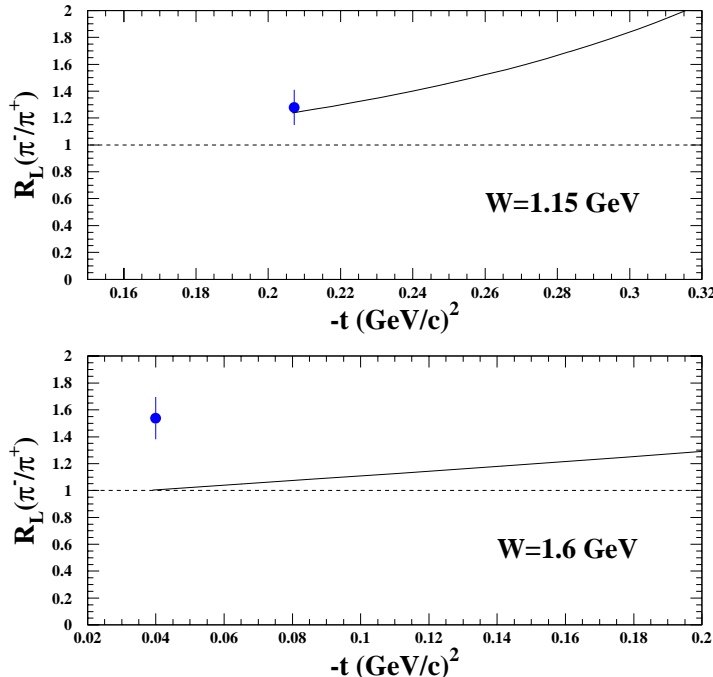


Fig. 7 Longitudinal  $\pi^-$  to  $\pi^+$  ratios from the first phase of experiment 91-003. The curve is the ratio as predicted by the MAID model of Drechsel et al <sup>7</sup>. At both kinematic settings, there is a clear deviation from one.

terms, a ratio of unity would indicate a lack of isoscalar backgrounds and give one some confidence that the pole process is indeed the dominant contribution to the longitudinal cross section. The kinematics for the initial phase of E91-003 were chosen so as to attempt to satisfy the above condition. However, preliminary analysis of the longitudinal  $\pi^-$  to  $\pi^+$  ratios indicate that there are non-negligible isoscalar backgrounds (see Fig. 7). Although the ratios are in the neighborhood of one, it is unclear how the deviation from unity maps to the size of the contributions from the isoscalar backgrounds. For the  $W = 1.15 \text{ GeV}$  data, theory can provide some guidance and calculations indicate that the pole term is about 50 – 70% (by amplitude) of the total longitudinal cross section. Unfortunately, the theory is less helpful for the  $W = 1.6 \text{ GeV}$  data, making the interpretation of the data more difficult. The proposed kinematics for the remainder of this experiment would alleviate this problem. Analysis of the data already taken during E93-021 indicates that the longitudinal  $\pi^-$  to  $\pi^+$  is within 10% of unity (see Fig. 8).

2000/05/19 11.48

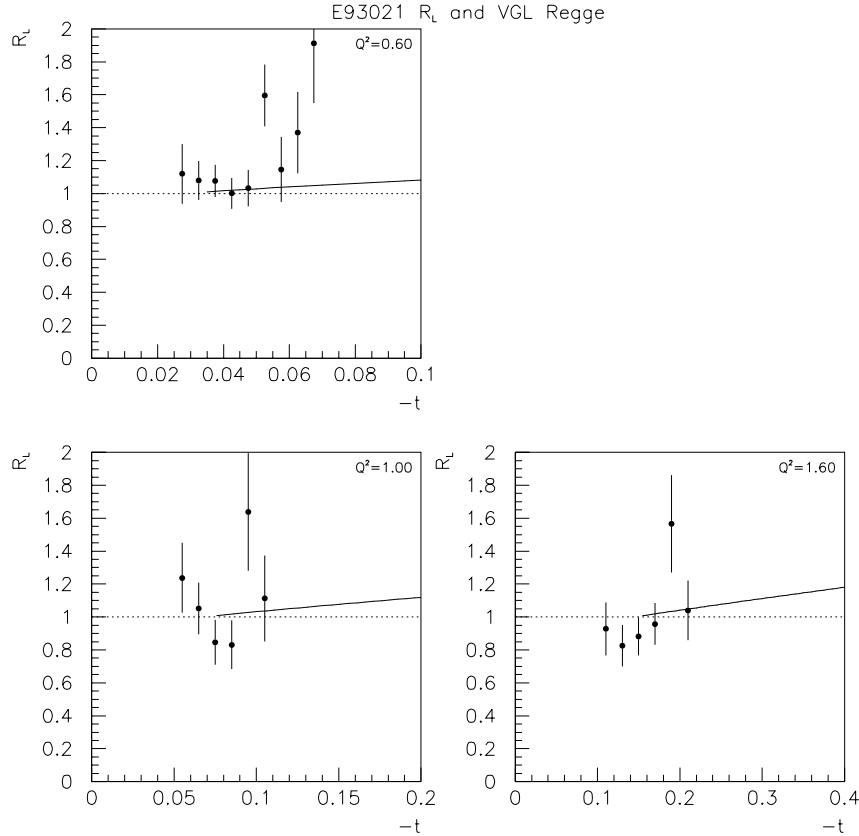


Fig. 8 Longitudinal  $\pi^-$  to  $\pi^+$  ratios from experiment 93-021. Closed circles are data and the curves are Regge calculations from Vanderhaeghen et al<sup>8</sup>. The data was taken at the kinematics proposed for this experiment. The points of primary interest are the  $Q^2 = 0.6 \text{ GeV}^2$  (upper left) and  $Q^2 = 1.6 \text{ GeV}^2$  (lower right) data. Figure courtesy of Vardan Tadevosyan for the  $F_\pi$  collaboration.

## 6 Runplan

In view of the considerations discussed above, we propose to complete the experiment by carrying out measurements at higher values of  $W$ , where we have more complete kinematic acceptance, and where we can take advantage of the data from E93-021 for the systematics

$W$ <i>GeV</i>	$Q^2$ <i>GeV<sup>2</sup></i>	$k_\pi$ <i>GeV</i>	$\epsilon$	E <i>GeV</i>	$P_{HMS}$ <i>GeV</i>	$\theta_{HMS}$ <i>deg.</i>	$P_{SOS}$ <i>GeV</i>	$\theta_{SOS}$ <i>deg.</i>	counts	I $\mu$ A	time hours
1.95	0.6	0.180	0.37	2.4	1.86	10.5	0.57	38.4	40k	100	35
1.95	0.6	0.180	0.75	3.6	1.86	15.2	1.77	17.5	40k	60	29
1.95	1.6	0.400	0.28	3.0	2.33	10.5	0.59	56.5	20k	100	112
1.95	1.6	0.400	0.63	4.0	2.33	16.6	1.63	28.5	40k	60	21
1.60	1.0	0.409	0.37	2.0	0.57	55.7	1.33	15.7	20k	100	108
1.60	1.0	0.409	0.92	5.0	3.57	13.6	1.33	28.8	40k	100	27
Total											332

Table 4: Kinematics for the proposed measurement.

of the cross section of the free proton. These kinematics have the additional advantages of high rates and low random coincidence backgrounds. Consequently, we have chosen a set of measurements at  $W = 1.95$  *GeV* corresponding to kinematics covered in the results of E93-021. In addition, we will carry out additional measurements at  $W = 1.6$  *GeV* for  $k_\pi \approx 400$  *MeV*. This, combined with the existing  $W = 1.6$  *GeV*,  $k_\pi \approx 200$  *MeV* data will provide measurements at low and high  $k_\pi$  for two values of  $W$ . The comparison of these data will provide a test of the validity of the assumptions made about the reaction mechanism. The kinematics of the proposed measurements are presented in Table 4 and the run plan in Table 5. Note that beam time estimates for the  $W = 1.95$  *GeV* points are based on Monte Carlo calculations that give rates that agree with the data already acquired during E93-021. Currents used for these rate estimates are taken from the actual running conditions during E93-021. Rates for the  $W = 1.6$  *GeV*,  $Q^2 = 1.0$  *GeV<sup>2</sup>* points were estimated using a model that agrees with data taken during E91-003 at  $W = 1.6$  *GeV* and  $Q^2 = 0.4$  *GeV<sup>2</sup>*.

## 7 Request for beam time

We request 400 hours of beam to complete the experiment. Note that two linac gradients (1.0 *GeV* per pass and 1.2 *GeV* per pass) are required for the kinematics as described above - time has been allotted in the beam time request to account for the necessary gradient change. In order to minimize the overhead in mounting the experiment and configuring the spectrometers, we suggest that the scheduling of measurements be coordinated with the running of the future phase of E91-021. The same cryotarget can be

Activity	Time hours
Production Running	332
Elastic Data	12
Linac Gradient Change	8
Beam Energy Changes	8
Target Changeovers	24
Target Boiling Studies	16
Checkout/Calibration	8
Total	408 (17 days)

Table 5: The run plan.

used in both experiments, and it may be feasible to interleave some of the measurements requested here with those planned for the extension of E93-021.

## Acknowledgements

The authors wish to thank Prof. Lothar Tiator, University of Mainz, for providing the MAID pion electroproduction programs which were incorporated in the SIMC simulations used in the data analysis. This work is supported by the U.S. Department of Energy and the National Science Foundation.

## References

1. B.L. Friman, V.R.Pandharipande, and R.B. Wiringa, Phys. Rev. Lett. **51**, 763 (1983).
2. H. Jung, and G.A. Miller, Phys. Rev. **C41**, 659 (1990).
3. G.F. Bertsch, L. Frankfurt, and M. Strikman, Science **259**, 773 (1993).
4. D.M.Alde et al., Phys. Rev. Lett. **64**, 2479 (1990).
5. G. Bardin et al., Nucl. Phys. **B120**, 45 (1977).
6. R. Gilman et al., Phys. Rev. Lett. **64**, 622 (1990).
7. D. Drechsel, O. Hanstein, S. S. Kamalov and L. Tiator, Nucl. Phys. **A645**, 145 (1999).
8. M. Vanderhaeghen, M. Guidal and J. M. Laget, Phys. Rev. **C57**, 1454 (1998).